Front. Earth Sci. 2019, 13(2): 430–443
https://doi.org/10.1007/s11707-018-0715-y

RESEARCH ARTICLE

Vegetation and soil wind erosion dynamics of sandstorm control programs in the agro-pastoral transitional zone of northern China

Zhitao WU (✉)[1], Mingyue WANG[1], Hong ZHANG[1,2], Ziqiang DU[1]

1 Institute of Loess Plateau, Shanxi University, Taiyuan 030006, China
2 College of Environmental & Resource Sciences, Shanxi University, Taiyuan 030006, China

© Higher Education Press and Springer-Verlag GmbH Germany, part of Springer Nature 2019

Abstract To combat soil erosion and desertification, large-scale sandstorm control programs have been put in place since 2000 in the agro-pastoral transitional zone of northern China. Vegetation dynamics as well as soil wind erosion control effects are very important for assessing the ecological success of sandstorm control programs in China. However, no comprehensive evaluation of vegetation dynamics and soil wind erosion control effects in this region has been achieved. In this study, we illustrate the vegetation and soil wind erosion dynamics of sandstorm control programs in the northern Shanxi Province using remote sensing data and soil wind erosion models. There was a significant increase in vegetation cover for 63.59% of the study area from 2001 to 2014 and a significant decrease for 2.00% of the study area. The normalized difference vegetation index (NDVI) showed that the largest increase occurred in autumn. Soil wind erosion mass decreased from 20.90 million tons in 2001 to 7.65 million tons in 2014. Compared with 2001, the soil wind erosion moduli were reduced by 43.05%, 36.16%, and 62.66% in 2005, 2010, and 2014, respectively. Spatially, soil wind erosion in most of the study area was alleviated between 2001 and 2014. The relationship between NDVI and soil wind erosion mass showed that the increased vegetation coverage reduced the soil wind erosion mass. In addition, wind was the main driving force behind the soil wind erosion dynamics. The results indicate that the vegetation coverage has increased and soil wind erosion mass has been reduced following the implementation of the sandstorm control programs. However, the ecological effects of the sandstorm control programs may vary over different periods. While the programs appear to be beneficial in the short term, there may be unintended consequences in the long term. Research on the sustainability of the ecological benefits of sandstorm control programs needs to be conducted in the future.

Keywords NDVI, soil wind erosion, ecological effects, ecological restoration program, northern Shanxi Province

1 Introduction

Desertification, which is expressed as a persistent reduction or loss of biological and economic productivity of land, has become one of the world's most serious ecological, environmental, and socioeconomic problems (Wang, 2014; Lamchin et al., 2016). For decades, China has been confronting this problem, particularly in the agro-pastoral transitional zone of northern China. To understand and combat the process of desertification, China has implemented a variety of sandstorm control programs or ecological restoration programs, such as the 'Three-North Shelterbelt Forest Project' (TNSFP), the 'Grain to Green Project' (GTGP), and the 'Beijing–Tianjin Sand Source Control Project' (BTSSCP) (Yin and Yin, 2010; Wu et al., 2014). There are several major types of desertification including aeolian desertification, soil and water erosion, and salinization. Due to the efforts of national and local governments, the desertification land area in China decreased from 2.67 million km^2 in 1999 to 2.61 million km^2 in 2014 (Tu et al., 2016). Following the implementation of ecological restoration programs, vegetation coverage and soil wind erosion mass changed. Therefore, assessing the vegetation coverage and soil wind erosion dynamics of sandstorm control programs has become a key topic in ecologically vulnerable areas.

Vegetation is a sensitive indicator of the ecological environment (Fensholt and Proud, 2012). In the regions

Received January 24, 2018; accepted May 5, 2018

E-mail: wuzhitao@sxu.edu.cn

where targeted ecological restoration programs were implemented, vegetation species and vegetation coverage changed. Hence, large-scale vegetation dynamics (either improvements or degradations) are used to evaluate the effectiveness of ecological restoration programs. With the development of remote sensing technology, vegetation restoration is always characterized using the normalized difference vegetation index (NDVI), net primary productivity (NPP), leaf area index (LAI), fraction of Photosynthetically Active Radiation absorbed by vegetation (fPAR), and Vegetation Coverage (VC) (Donohue et al., 2009). Because the NDVI is positively correlated with the other factors, long-term NDVI is often used to monitor vegetation dynamics. For example, by using advanced very-high-resolution radiometer (AVHRR) NDVI data (He et al., 2015), it was observed that the overall state of vegetation improved under the TNSFP from 1982 to 2011. Moreover, some researchers used MODIS NDVI data to monitor the dynamics of vegetation activity and evaluate the effectiveness of ecological programs in Inner Mongolia from 2000 to 2012. An overall greening trend was found. They also found a significant increase in the NDVI for 15.38% of the study area, 5.67% of which resulted from by ecological restoration programs (Tian et al., 2015).

One of the aims of sandstorm control programs is to reduce soil wind erosion mass and thus restore the service functions of regional ecosystems (Zhang et al., 2016; Wang et al., 2017a). Soil wind erosion mass is calculated using the wind erosion equation (WEQ) (Woodruff and Siddoway, 1965) or a wind erosion model, such as RWEQ (Revised Wind Erosion Equation Model), TEAM (Texas Erosion Analysis Model), WEAM (Wind Erosion Assessment Model), or WEPS (Wind Erosion Prediction System) (Hagen, 1991; Shao et al., 1994; Fryrear et al., 1998; Gregory et al., 2004). Most of these empirical or process-based wind erosion models were developed for a field-sized scale. Although the parameters of these models have been tested in practice, it is difficult to apply them at a regional scale due to high parameter heterogeneity (Nan et al., 2013). The combination of remote sensing (RS), Geographic Information System (GIS), and Global Positioning System (GPS) technologies and wind tunnel experiments makes it possible to study the dynamics of soil wind erosion at the regional scale. Some studies have demonstrated the spatiotemporal dynamics of soil wind erosion mass in regional sandstorm control programs. In China, a regional soil wind erosion model was developed using wind tunnel experiments, RS, GIS, and GPS technologies, which is suitable for the arid and semi-arid conditions of northern China (Gao et al., 2012). At present, this model has been applied in the national water conservancy survey. Moreover, this model has been used to assess the ecological benefits of the 'Beijing–Tianjin Sand Source Control Project' at the regional scale.

Under the impacts of climate change and large-scale human activities, the effectiveness of regional sandstorm control programs may vary in China. Many studies have found that desertification and dust storms were controlled following the implementation of these programs. In addition, the overall ecosystem service function has been improving in the affected regions (Zhang et al., 2000; He et al., 2015). For example, the effectiveness of the Beijing-Tianjin Sand Source Control Project was assessed using vegetation dynamics. Vegetation coverage and NDVI have increased since the implementation of the restoration program (Wu et al., 2013). Also, the 'Natural Forest Conservation Program' and the 'Grain to Green Program' increased vegetation cover, enhanced carbon sequestration, and reduced dust to other countries by controlling soil erosion (Liu et al., 2008). Nevertheless, several experts have claimed that the effectiveness of sandstorm control programs in northern China or semi-arid and arid regions may be overestimated (Wang et al., 2010). They generally agree that key measures such as afforestation and the planting of grass combat and prevent desertification. However, regional soil attributes and ecological conditions are not suitable for the survival of the vegetation species used in these measures. Some experts have further asserted that desertification will expand and that afforestation could increase wind erosion and lead to the degradation of ecological environment (Cao, 2008).

Northern Shanxi Province is located in the agro-pastoral transitional zone of northern China. Aeolian desertification, which is defined as land degradation through wind erosion, is a major environmental problem impeding local development. The area of desertified land resulting from wind erosion was 617.79 km^2, accounting for 25.14% of the total land in northern Shanxi Province (Du et al., 2016). To combat aeolian desertification, large-scale ecological restoration programs were implemented after 2000 in this region including the "Beijing-Tianjin Sand Source Control Programs", the fourth phase of the "Three-north Shelterbelt Forest Construction Project", the "Natural Forest Conservation program", and the "Grain to Green Project". Because this region is an important part of the Loess Plateau and the "golden triangle" of Shanxi-Shaanxi-Inner Mongolia, it is essential to rigorously evaluate the vegetation and soil wind erosion dynamics of these programs. The change in annual and seasonal vegetation coverage and soil wind erosion mass over the last 15 years needs to be evaluated. Furthermore, broader application of these programs with the aim of improving the regional vegetation and decreasing soil wind erosion across northern Shanxi needs to be determined. These points have important implications for policy makers for future ecological restoration works. In this study, based on remote sensing and model simulation data, we (i) illustrate the vegetation and soil wind erosion dynamics of sandstorm control programs in the northern Shanxi Province, (ii) analyze the interannual variation of NDVI and soil wind erosion mass from 2000 to 2014, and (iii) assess the possible impact of wind on ecological effects.

2 Study area and dataset

2.1 Study area

The study area is bounded by Pianguan County to the west, Fanshi County to the east, Baode County to the south, and Tianzhen County to the north. This area lies between 111°55′E–114°31′E and 38°39′N–40°43′N (Fig. 1). There are 20 counties in this region with a total area of about 31,800 km^2. The area is the most important part of the Loess Plateau in China. In addition, most mineral and other natural resources in Shanxi Province are located in this region. The study area is characterized by a temperate continental monsoon climate with dry and cold winters and windy springs. The mean annual temperature is between 3.6°C and 8.8°C, with a record low of –40.4°C and record high of 38.8°C. The mean annual precipitation ranges from 350 to 500 mm and mainly falls between July and September. The mean annual evaporation is approximately 1700 to 2300 mm. The mean annual wind velocity is more than 4.0 m/s, and there are more than 20 gale days per year. Wind velocity reaches 17–21 m/s, usually in the period from March to May. The study area is a transitional zone between warm temperate deciduous forest and temperate grassland. The main vegetation types are secondary scrubs and grasses (Xue et al., 2013; Du et al., 2016; Xu et al., 2016).

2.2 Dataset and methods

2.2.1 Dataset

The monthly NDVI data, with 1 km and 250 m spatial resolutions covering the period from 2000 to 2014, were derived from the Moderate Resolution Imaging Spectroradiometer (MODIS) on the National Aeronautics and Space Administration (NASA) Earth Observing System (EOS) satellite. Monthly MODIS NDVI data were obtained using the Maximum Value Composite (MVC) method, which minimizes cloud contamination, atmospheric effects and solar zenith angle effects (Holben, 1986). Ground conditions strongly affect NDVI, leading to unstable values that cannot accurately represent vegetation status in desert regions (Fang et al., 2004). The monthly NDVI data with 1 km spatial resolution was analyzed for vegetation dynamics. The monthly NDVI data with 250 m spatial resolution was analyzed for soil wind erosion dynamics. In this study, an NDVI threshold of 0.05 was used to exclude bare and sparsely vegetated areas (Slayback et al., 2003; Wang et al., 2011). The land use data for northern Shanxi for 2000 and 2010 was obtained by using Thematic Mapper (TM) and Enhanced Thematic Mapper Plus (ETM+) sensors from Landsat satellite images. After preprocessing procedures, we integrated unsupervised classification and visual interpretation to extract land use information (Xu et al., 2016).

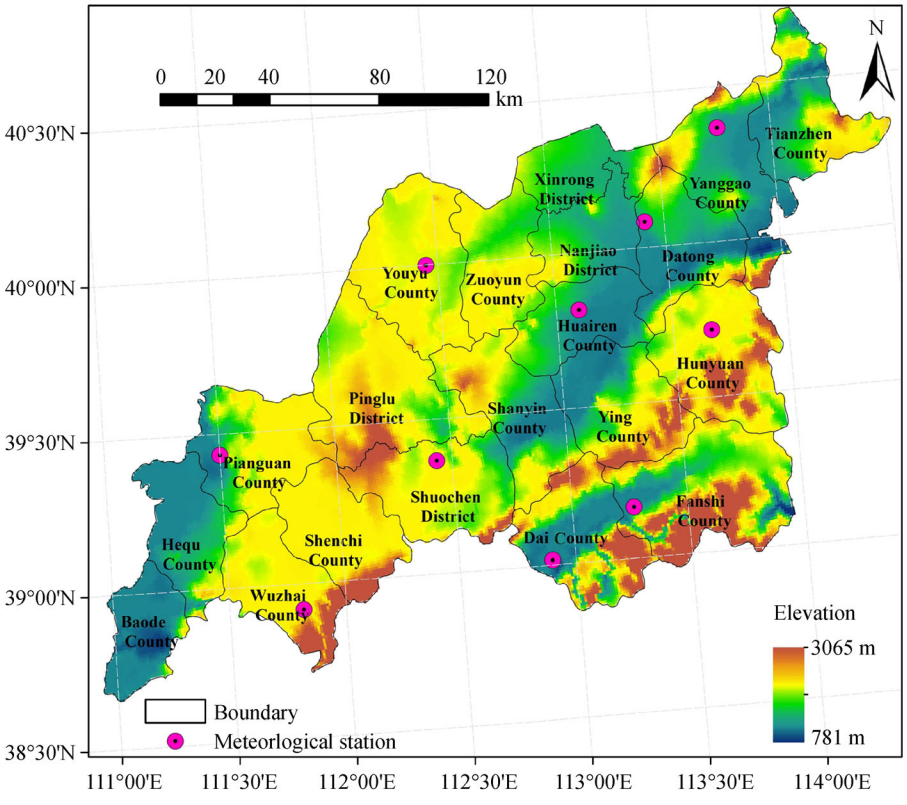

Fig. 1 Location of the study area.

The NDVI trends in the time series were detected using a linear regression method (LRM). The slope of the regression indicates the mean temporal change in the NDVI. Positive slopes indicate increasing trends, while negative slopes indicate decreasing trends. The relative change (increase or decrease) in the rate of vegetation during the study period was estimated as follows (Piao et al., 2003; Wu et al., 2013):

$$\mathrm{RCR} = slope/mean \times N \times 100\%, \tag{1}$$

where RCR is the relative change rate, *slope* is the slope of NDVI, *mean* is the average NDVI over N years, and N is the length of the study period.

2.2.2 Model for soil wind erosion mass

In this study, the soil wind erosion mass was evaluated based on a regional soil wind erosion model (Gao et al., 2012). This model includes three sub-models with different land use types. In this study, because the land use types are mainly cultivated land, forest, and grassland, we chose two sub-models to analyze the soil wind erosion change in northern Shanxi Province.

First, for the cultivated land, the soil wind erosion modulus is computed as follows:

$$Q_a = 10 \times C \times \sum_{j=1} \left\langle T_j \times \exp\left\{ a_1 + \frac{b_1}{z_0} + c_1 \times \left[(A \times U_j)^{0.5} \right] \right\} \right\rangle, \tag{2}$$

where, Q_a is the soil wind erosion modulus [t/(hm^2·yr)] for the cultivated land. U_j is the j^{th} level wind velocity taken from meteorological stations. This value is higher than the critical wind velocity that leads to soil wind erosion. In northern China, the critical wind velocity is always 5.0 m/s for farmlands. The average of the j^{th} level wind velocities is selected. For example, the wind velocity at meteorological stations is measured to be between 5.0 and 6.0 m/s, resulting in a U_j of 5.5 m/s. Therefore, $U_{j=1}$ = 5.5 m/s, $U_{j=2}$ = 6.5 m/s, and so on. T_j is the cumulative time of U_j (min); A is the correction coefficient of wind velocity equal to about 0.893; z_0 is the surface roughness (cm) of about 0.55 cm; C is a constant (0.0018); and a_1, b_1, and c_1 are the regression coefficients with the values of –9.208, 0.018, and 1.955, respectively.

Secondly, for the forest or grassland, the soil wind erosion modulus is calculated as follows:

$$Q_b = 10 \times C \times \sum_{j=1} \left\langle T_j \times \exp[a_2 + b_2 \times \mathrm{VC}^2 + c_2/(A \times U_j)] \right\rangle, \tag{3}$$

where, Q_b is the soil wind erosion modulus [t/(hm^2·yr)] for the forest or grassland; VC is the vegetation coverage; and a_2, b_2, and c_2 are the regression coefficients with the values of 2.4869, –0.0014, and –54.9472, respectively. C, U_j, T_j, and A in Eq. (3) have the same meanings as in Eq. (2). The wind velocities that can lead to soil wind erosion for different vegetation coverage levels are shown in Table 1.

Based on the Eqs. (2) and (3), the soil wind erosion modulus at the i^{th} pixel is calculated as follows:

$$Q_i = \begin{cases} Q_{a\_i} & \text{the land type of } i^{\text{th}} \text{ pixel is cultivated land} \\ Q_{b\_i} & \text{the land type of } i^{\text{th}} \text{ pixel is forest or grassland} \end{cases}, \tag{4}$$

where, Q_i is the soil erosion modulus at the i^{th} pixel [t/(hm^2·yr)]; and Q_{a_i} and Q_{b_i} are the soil wind erosion modulus of i^{th} pixel with respect to cultivated land and forest or grassland.

The regional total soil wind erosion modulus is obtained by summing the soil erosion moduli for all pixels. Then, the soil wind erosion mass is obtained as follows:

$$Q_{\text{total}} = S \times \sum_{i=1}^{n} Q_i, \tag{5}$$

Table 1 Wind velocity leading to soil wind erosion for different vegetation coverage levels

Vegetation coverage/%	Mean vegetation coverage/%	Wind tunnel wind velocity/(m·s^{-1})	Meteorological station wind velocity/(m·s^{-1})	$U_{j=1}$/(m·s^{-1})	
				Range	Average
0–5	2.5	7.30	8.20	8–9	8.5
5–10	7.5	7.54	8.47	8–9	8.5
10–20	15.0	7.97	8.95	8–9	8.2
20–30	25.0	8.68	9.75	9–10	9.5
30–40	35.0	9.60	9.60	10–11	10.5
40–50	45.0	10.79	10.79	12–13	12.5
50–60	55.0	12.33	12.33	13–14	13.5
60–70	65.0	14.03	14.03	15–16	15.5

where, Q_{total} is the regional soil wind erosion mass (t/yr); and S is the area of each pixel area (hm^2). In this study, the area of each pixel is 6.25 hm^2.

In this study, vegetation coverage from 2001 to 2014 was calculated using a dimidiate pixel model (Chen et al., 2001). Hourly wind velocity data from 10 meteorological stations distributed throughout the study area were obtained from the Shanxi Meteorological Center, China. According to the dust data from these stations, the dust, which resulted from soil wind erosion, was rarely present in the northern Shanxi Province for the months of July, August, and September. In addition, due to the higher vegetation coverage, wind soil erosion was very weak during these months. Therefore, the cumulative time for wind velocity was set for the entire year minus these three months. The cumulative hours for wind velocity for different levels are shown in Table 2. We found that the cumulative hours of wind velocity at different meteorological stations varied. For example, in 2005 in Yanggao County, the total number of hours for a 5–6 m/s wind velocity was 421 hours, while the total was only 130 hours in Pianguan County. Moreover, there was a large difference between the wind velocities at the two adjacent meteorological stations: again in 2005, the total hours of a 7–8 m/s wind velocity in Youyu County was 107 compared to only 5 hours in Pianguan County. To solve these problems, the cumulative time for the wind data was interpolated grids by inverse distance weighted interpolation method with a chosen size of 250 meters. Figure 2 shows the spatial patterns of the cumulative time for the wind at different levels from January to December (except July, August, and September) in 2005 in the northern Shanxi Province.

A classification of soil erosion intensity is provided in Table 3, which was obtained from the Ministry of Water Resources of China.

3 Results

3.1 Vegetation dynamics in northern Shanxi Province

3.1.1 Northern Shanxi wide trend analysis

NDVI trends were evaluated at annual and seasonal scales using an LRM for 2000–2014. Because the winter snow

Table 2 Cumulative hours of wind for meteorological stations at different level from January to December (except July, August, and September) in 2005 and 2010

Year	Wind/($m \cdot s^{-1}$)	Cumulative hours of wind									
		Yanggao	Datong	Hunyuan	Huairen	Youyu	Pianguan	Shuochen	Wuzhai	Daixian	Fanshi
2005	5–6	421	394	244	332	321	130	246	278	315	197
	6–7	215	257	142	180	201	62	149	217	142	89
	7–8	109	121	91	131	107	5	101	115	76	56
	8–9	35	75	47	68	63	1	44	67	37	17
	9–10	11	26	27	14	26	0	16	33	19	5
	10–11	1	3	3	4	9	0	2	12	9	3
	11–12	0	2	1	1	0	0	1	4	2	1
	12–13	0	1	1	0	0	0	0	4	0	0
	13–14	0	0	0	0	0	0	0	1	0	0
	14–15	0	0	0	0	0	0	0	1	0	0
	15–16	0	0	0	0	0	0	0	0	0	0
2010	5–6	394	467	468	280	352	161	231	468	286	206
	6–7	181	312	240	134	218	53	169	240	127	105
	7–8	90	174	100	61	131	15	66	100	61	32
	8–9	39	83	60	33	58	5	38	60	36	14
	9–10	15	32	26	15	20	3	7	26	18	3
	10–11	9	11	12	6	7	0	3	12	10	2
	11–12	4	6	5	4	2	0	0	5	1	0
	12–13	1	2	3	5	2	0	2	3	3	0
	13–14	2	1	2	3	2	0	1	2	1	0
	14–15	1	0	1	0	0	0	0	1	1	0
	15–16	0	0	0	0	1	0	1	0	1	0

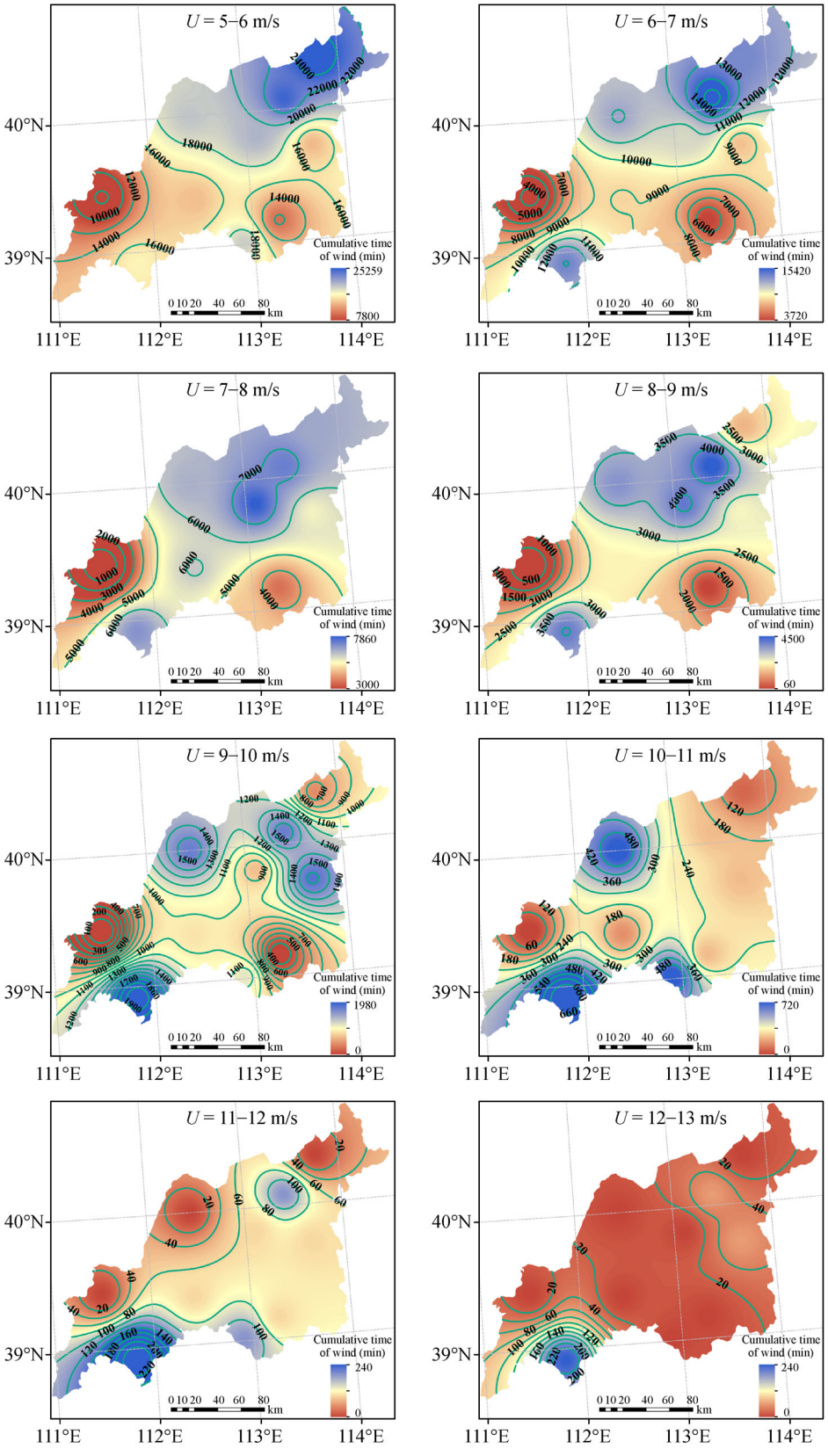

Fig. 2 Spatial patterns of the cumulative time of wind at different levels from January to December (except July, August, and September) in 2005 in the northern Shanxi Province (min).

Table 3 Classification of soil erosion intensity

Level	Wind erosion modulus/(t·hm^{-2}·yr^{-1})
Micro	< 2
Mild	2–25
Moderate	25–50
Strength	50–80
Strong	80–150
Severe	> 150

influences the NDVI value, we analyzed the seasonal NDVI for three seasons: spring (March to May), summer (June to August), and autumn (September to November). For the 2000–2014 period, a statistically significant positive trend in the annual NDVI was observed (0.0035 yr^{-1}, R^2= 0.56, P = 0.001) (Fig. 3). At the regional scale, the maximum annual NDVI appeared in 2013 while the minimum value was found in 2001. The change in the annual NDVI trend was largely contributed by three seasonal NDVI changes. More specifically, the largest NDVI increase occurred in the autumn (R^2= 0.80, P < 0.001), with a magnitude of 22.03% over the 15 years and a trend of 0.0047 yr^{-1}. The 15-year mean NDVI was 0.32. The rates of increase for summer and spring were 21.70% and 21.00%, respectively, having trends of 0.0068 yr^{-1} (R^2= 0.37, P = 0.017) and 0.0028 yr^{-1} (R^2= 0.61, P = 0.001) (Table 4). Although the NDVI increased in all the three seasons, several large fluctuations appeared in the NDVI trends. For example, the summer NDVI reached a peak in 2013 but was lower in 2001 and 2009, while the spring NDVI was large in 2014 but small in 2001. Additionally, summer is the best season for vegetation growth, and therefore, the patterns of the summer NDVI variations corresponded well with those of the annual NDVI. Generally, the vegetation cover has increased at the annual and seasonal scales since the implementation of sandstorm control programs 15 years ago.

3.1.2 Spatial patterns of annual and seasonal NDVI trends

By extracting the annual and seasonal mean NDVI, the spatial patterns of the linear trends in annual and seasonal NDVI were calculated (Fig. 4). Overall, the annual NDVI trend for 91.58% of the total study area increased during 2000–2014 and the trend for 63.59% of the study area was pass significant test (p < 0.05) (Table 5). The NDVI increased in the southwest, especially in Baode and Wuzhai Counties, in the central region in Youyu, Zuoyun, and Huairen Counties, and northeast in Tianzhen and Yanggao Counties, while it decreased sharply in the center of the Nanjiao district, south of Fanshi County, and north of the Shuochen district (Fig. 4(d)). Furthermore, the spatial patterns of the seasonal NDVI change were spatially heterogeneous (Figs. 4(a)–4(c)). For most of the study area, the three seasonal NDVI trends were positive,

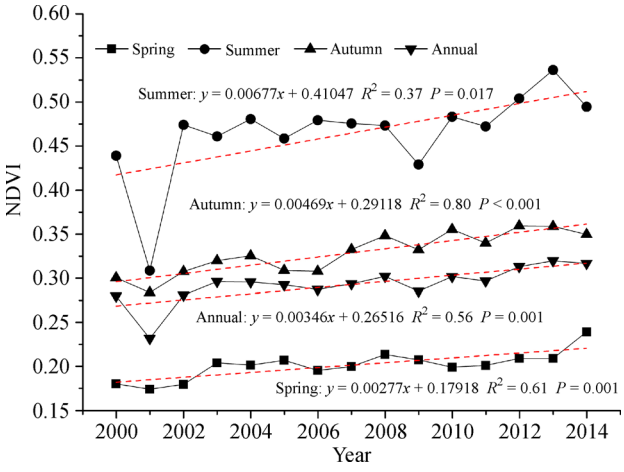

Fig. 3 Interannual variation in seasonal and annual NDVI in the northern Shanxi Province from 2000 to 2014.

Table 4 Mean value, trend, and relative increase rate of annual and seasonal NDVI

Season	Mean±SD	Trend per year	Relative increase/%
Spring	0.20±0.0158	0.0028	21.00
Summer	0.47±0.0501	0.0068	21.70
Autumn	0.32±0.0235	0.0047	22.03
Annual	0.29±0.0208	0.0035	18.10

but they decreased in a small area south of Fanshi County and in the center of Nanjiao district. The increasing NDVI throughout the three seasons contributed to the increase in annual NDVI that occurred in most areas of northern Shanxi Province. In contrast, the combined decrease in the summer and autumn NDVI in Fanshi County and the Nanjiao district resulted in a sharp decrease in annual NDVI (Fig. 4(d)). We summarized the percentage of seasonal NDVI increase or decrease at 0.95 confidence levels across the study area. Over the past 15 years, the largest NDVI increase occurred in the autumn, while the smallest increase was in the spring. Statistically, 92.83% of the total study area had an increase in NDVI in autumn over the 15 years, of which 67.03% had a significant increase at 0.95 confidence level, while the values in the spring and summer were, respectively, 92.55% (66.13% at 0.95 confidence level) and 92.49% (49.22% at 0.95 confidence level).

3.2 Soil wind erosion dynamics in the northern Shanxi Province

3.2.1 Interannual variation in soil wind erosion

Because it is difficult to obtain all the hourly wind velocity data of 10 meteorological stations from 2001 to 2014, we only calculate the soil wind erosion masses and moduli for

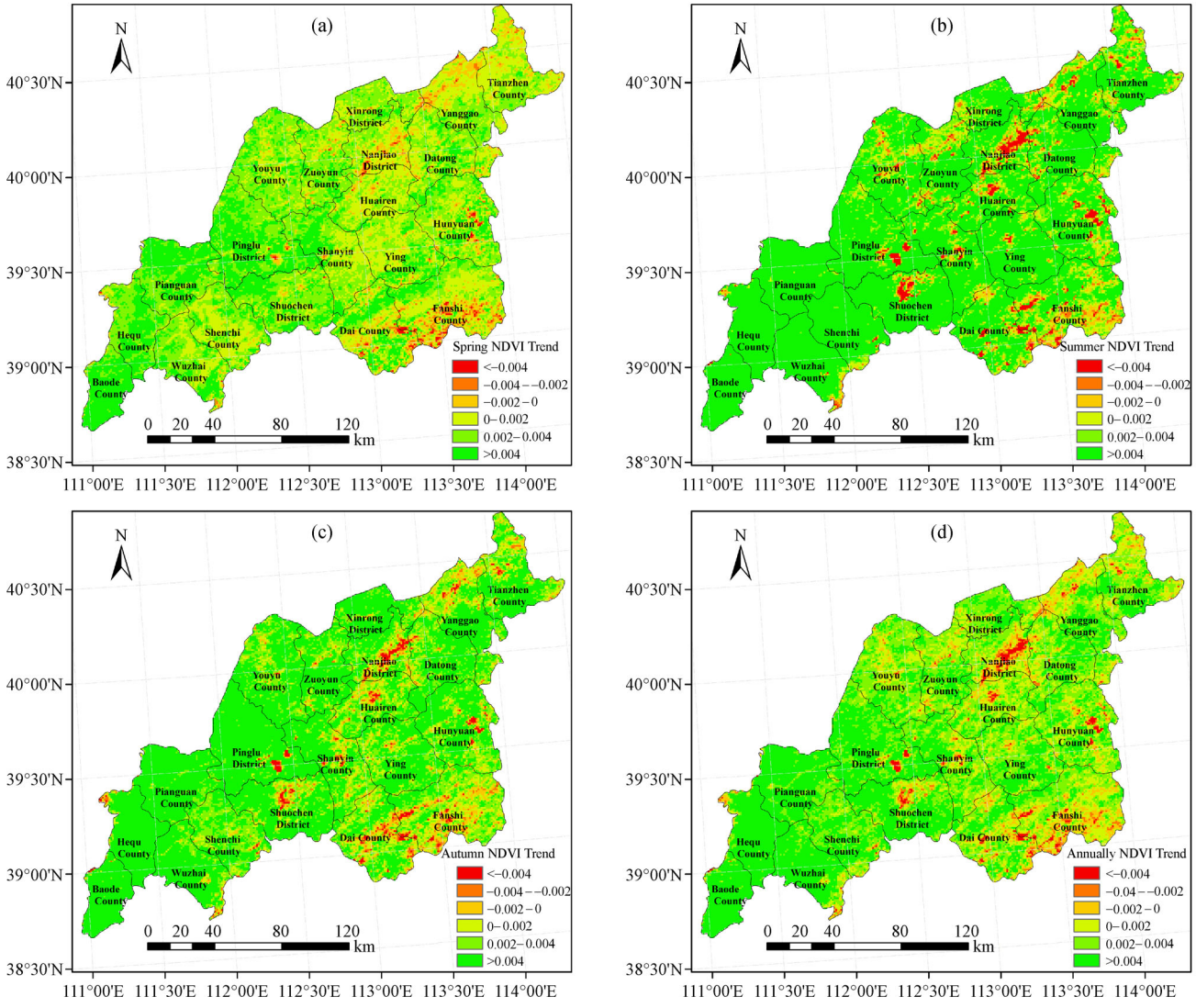

Fig. 4 Spatial patterns of NDVI trends for each grid cell for (a) spring (Mar.–May), (b) summer (Jun.–Aug.), (c) autumn (Sept.–Nov.), and (d) annually (Jan.–Dec.) over the period 2000–2014 in northern Shanxi Province.

Table 5 Percentage of NDVI increase/decrease at 0.95 confidence levels for the year and different seasons in northern Shanxi Province

Season	Significant increase/%	Non-significant increase/%	Non-significant decrease/%	Significant decrease/%
Spring	66.13	26.42	6.64	0.81
Summer	49.22	43.27	6.09	1.42
Autumn	67.03	25.80	5.93	1.24
Annual	63.59	27.99	6.42	2.00

the years 2001, 2005, 2010, and 2014 based on the regional soil wind erosion model. Interannual variations in soil wind erosion mass and modulus are shown in Fig. 5. For all years the soil erosion mass and modulus decreased in northern Shanxi Province. Specifically, the soil wind erosion masses were 20.9, 11.89, 13.11, and 7.65 Mt in 2001, 2005, 2010, and 2014, respectively. The mean soil erosion moduli were 6.83, 3.89, 4.36, and 2.55 t/(hm^2·yr) in 2001, 2005, 2010, and 2014, respectively. Compared with 2001, the soil wind erosion mass was reduced by 43.11%, 34.27%, and 63.40% in 2005, 2010, and 2014, respectively. Similarly, compared to 2001, the soil wind erosion moduli were reduced by 43.05%, 36.16%, and 62.66% in 2005, 2010, and 2014, respectively. Hence, the

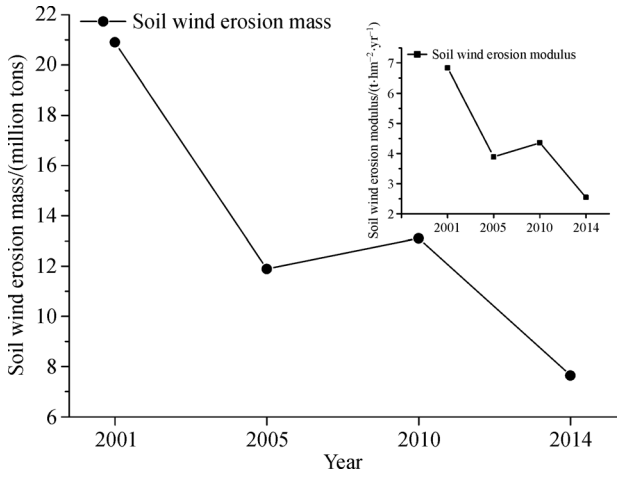

Fig. 5 Interannual variations in soil wind erosion mass and modulus in 2001, 2005, 2010, and 2014.

implementation of sandstorm control programs had a positive impact on controlling soil wind erosion.

3.2.2 Spatial patterns of soil wind erosion

We also analyzed the spatial distribution of soil wind erosion intensity (modulus) in the northern Shanxi Province. The spatial distribution of the soil wind erosion moduli for 2001, 2005, 2010, and 2014 is shown in Fig. 6. Here, red represents the largest soil wind erosion modulus while green represents the smallest soil wind erosion modulus. In 2001, the soil wind erosion modulus was more than 8 t/($hm^2 \cdot yr$) in most areas of northern Shanxi Province. The region with a high modulus (>10 t/($hm^2 \cdot yr$)) was distributed across a southwest-northeast strip that included Tianzhen, Datong, Huairen, Ying, Shenchi, and Wuzhai Counties and the Shuocheng district. In 2005, the soil wind erosion modulus was less than 8 t/($hm^2 \cdot yr$) for most of the study area. The high modulus region (>10 t/($hm^2 \cdot yr$)) was mainly distributed across parts of Wuzhai and Datong Counties and the Nanjiao district. In 2010, the soil wind erosion modulus was larger than in 2005. The high modulus region (>10 t/($hm^2 \cdot yr$)) was mainly distributed northeast of the study area and in Wuzhai County. However, in 2014, the soil wind erosion modulus in most areas had dropped to less than 6 t/($hm^2 \cdot yr$). The high modulus region (>10 t/($hm^2 \cdot yr$)) was only distributed in Datong and Hunyuan Counties. Moreover, we found that 76.47% of the study area was dominated by mild wind erosion in 2001. However, with the implementation of ecological programs, the study area was primarily dominated by micro wind erosion in 2005, 2010, and 2014. The area percentages exhibiting mild wind erosion were 76.47%, 52.84%, 53.13%, and 53.84% in 2001, 2005, 2010, and 2014, respectively (Table 6).

3.3 Relationship between vegetation coverage and soil wind erosion mass

In this section, to illustrate the relationship between NDVI and wind erosion mass, we analyze the spatial distribution of vegetation coverage in northern Shanxi Province. The spatial distribution of vegetation coverage in 2001, 2005, 2010, and 2014 is shown in Fig. 7. Red represents the lowest vegetation coverage while green represents the largest vegetation coverage. The spatial distribution of vegetation coverage had a negative correlation with the spatial distribution of soil wind mass. In 2001, 2005, 2010, and 2014, the vegetation coverage was relatively low, coinciding with peaks in the soil wind erosion mass. The vegetation coverage in 2005, 2010, and 2014 was higher than that in 2001 (Fig. 7). In particular, in 2001, vegetation coverage ranged from 5% to 25% in most areas of northern Shanxi Province. Similarly, the soil wind erosion modulus in 2001 was more than 8 t/($hm^2 \cdot yr$) in most of the study area. In 2005, vegetation coverage ranged from 25% to 50% in most areas of northern Shanxi province. The soil wind erosion modulus was less than 8 t/($hm^2 \cdot yr$) in most of the study area. In 2010, vegetation coverage was smaller than that in 2005 and the soil wind erosion modulus was larger than for 2005. However, in 2014, the vegetation coverage in most of study area was higher than in other years. And the soil wind erosion modulus in most areas had dropped to less than 6 t/($hm^2 \cdot yr$). In addition, the soil wind mass in 2014 was the lowest in four years. Therefore, the increased vegetation coverage had alleviated the soil wind erosion mass.

4 Discussion

4.1 Vegetation dynamics and soil wind erosion control effects of sandstorm control programs

Positive NDVI trends were found in most areas of the northern Shanxi Province, 91.58% of the total area, and 63.59% at a 0.95 confidence level over the 15 years. Our findings are consistent with those of many previous studies based on remote sensing data and field investigation data (Wu et al., 2012). For example, the NDVI increased from 2000 to 2012 in the northern Shanxi Province based on MODIS NDVI data (Zhu, 2014). Similarly, by combining MODIS NDVI data and detailed field investigation data, an increasing trend in vegetation coverage between 2001 and 2010 was documented (Gao et al., 2012). Moreover, the net primary productivity (NPP) showed an increasing trend in northern Shanxi Province from 2000 to 2014. Here, the NDVI positively correlated with NPP and vegetation coverage (Shen, 2016). An increase in NDVI after the implementation of sandstorm control programs suggests that these programs have also enhanced carbon

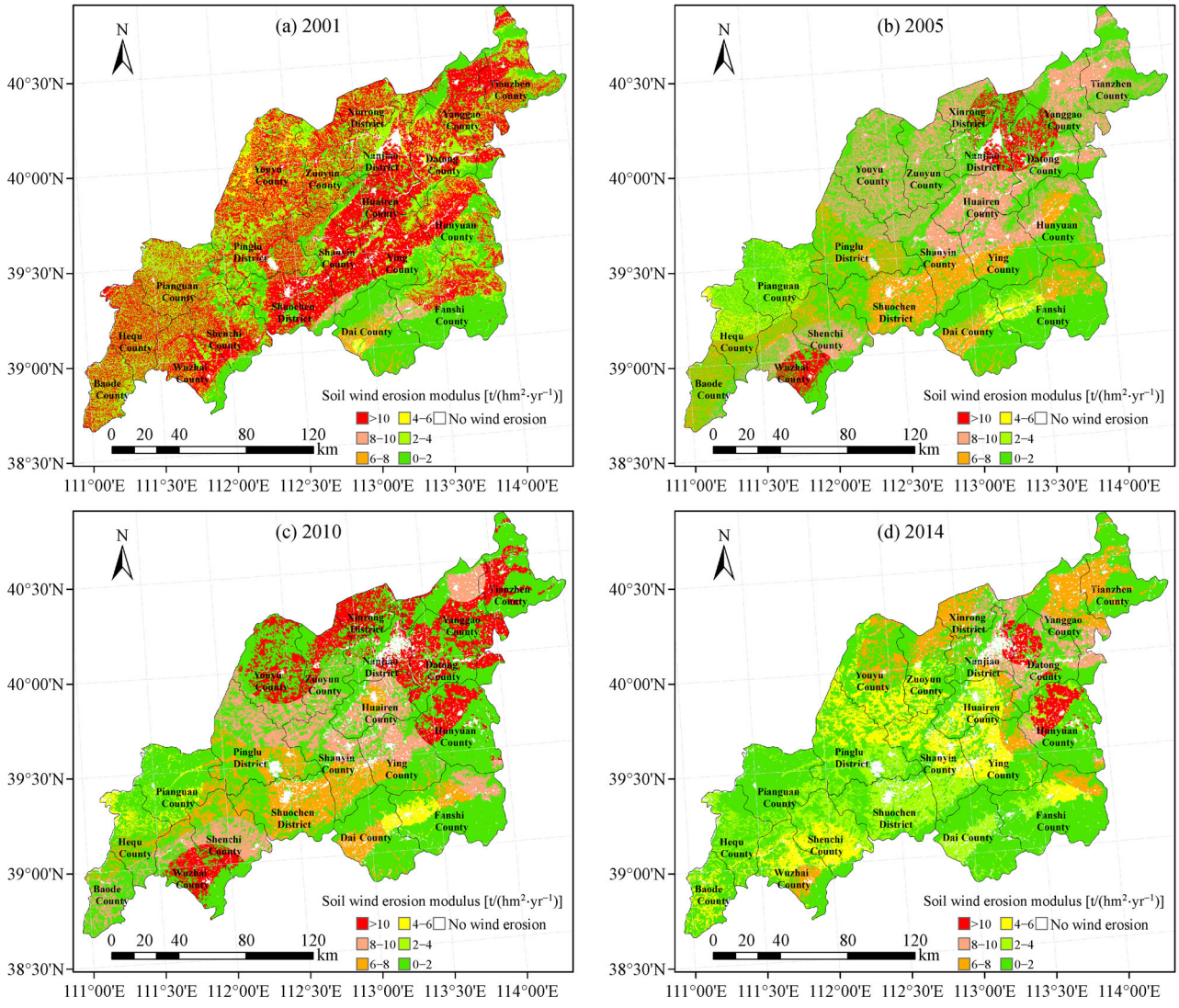

Fig. 6 Spatial distribution of soil wind erosion modulus for 2001, 2005, 2010, and 2014 in the northern Shanxi Province.

Table 6 Area percentage of soil wind erosion degrees areas for 2001, 2005, 2010, and 2014 in northern Shanxi Province (%)

Year	No wind erosion	Micro	Mild
2001	3.66	19.88	76.47
2005	3.66	52.48	43.86
2010	5.28	53.13	41.59
2014	5.28	53.48	41.24

sequestration and increased vegetation coverage in northern Shanxi Province. For example, the areas that were converted from croplands to forests under the Grain to Green Program will be able to sequester 110.45 Tg C by 2020 in China (Liu et al., 2014). Furthermore, the total carbon storage under the Henan Province's Grain to Green Program was 51.73 Tg in 2012 (Wang et al., 2017b). Therefore, the vegetation restoration in northern Shanxi Province after 2000 has also been beneficial to mitigating increases in atmospheric greenhouse gases.

After the sandstorm control programs were implemented in northern Shanxi Province in 2001, the soil wind erosion mass in the region had declined by 63.40% by 2014. Some studies have shown that ecological restoration programs can reduce regional soil wind erosion (Deng et al., 2012; Webb et al., 2016). In China, for instance, the Grain to Green Project reduced soil erosion by 45.4% based on a comparison of two periods, 2003–2007 and 1998–2002 (Deng et al., 2012). After the implementation of the Natural Forest Conservation Program, Liu also found that the area suffering from soil erosion declined by 6% between 1998 and 2003 in the upper and middle reaches of the Yangtze and Yellow River basins (Liu et al., 2008). Therefore, following the implementation of sandstorm control programs in 2000, regional vegetation cover increased and dust was reduced by the control of soil

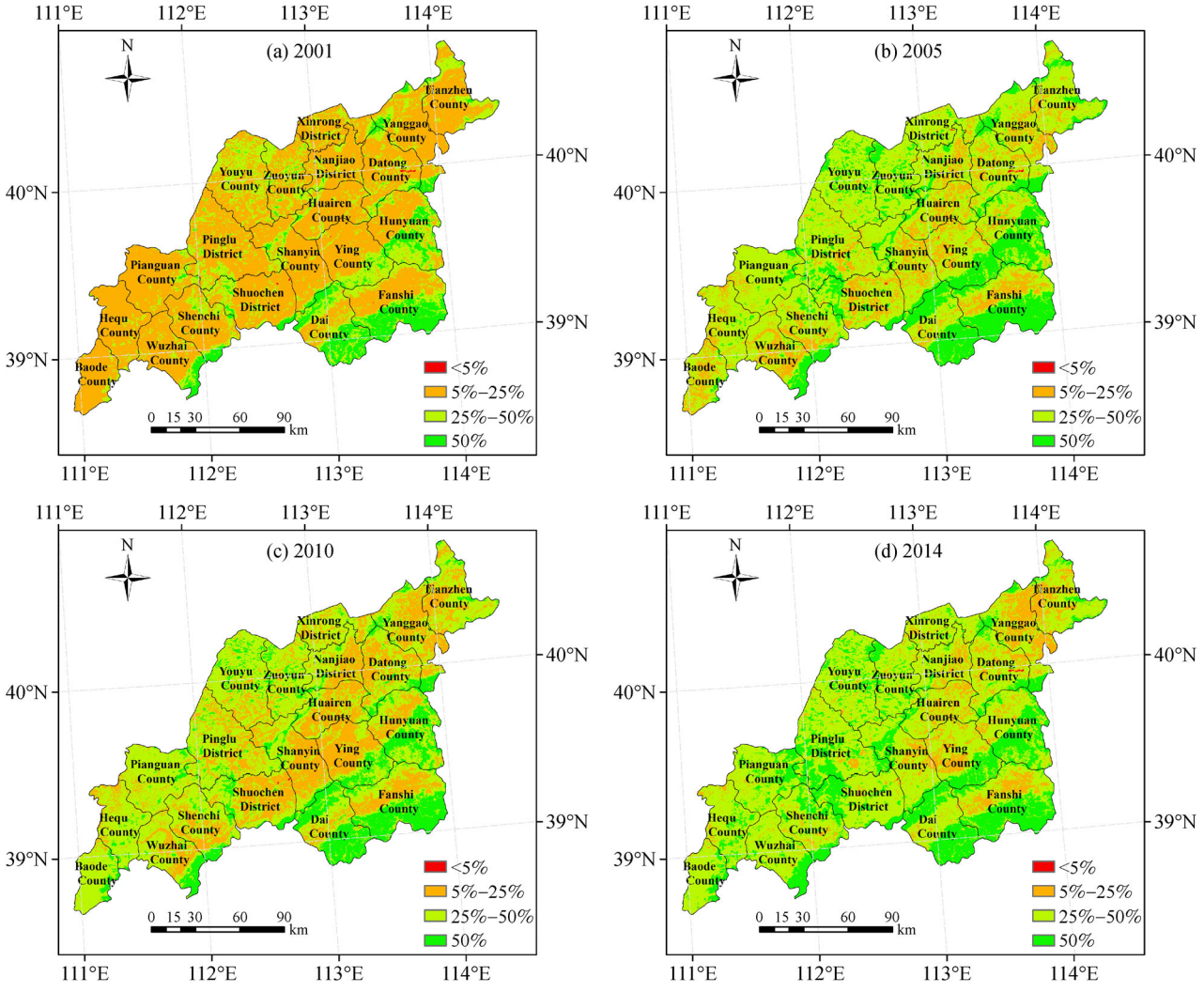

Fig. 7 Spatial distribution of vegetation coverage in 2001, 2005, 2010, and 2014.

erosion. However, the effectiveness of ecological restoration programs is complex. Ecological effects may be beneficial in the short term but may have unexpected consequences in the long term. In the short term, the impact of human activities on ecological effects is greater than the impact of natural factors in these regions. However, in recent years, the frequency of extreme climate events has increased. The influence of extreme climate events on ecological effects may become more detrimental than that of human activities. Research on the sustainability of ecological benefits of sandstorm control programs needs to be conducted in the future.

4.2 Impacts of wind on soil wind erosion mass

As the fundamental driving force of soil wind erosion, the interannual wind change has a large influence on the soil wind erosion mass change. Increased wind can aggravate the intensity of soil wind erosion and vice-versa (Liu et al., 2007; Pi et al., 2017). In this section, we discuss the relationship between cumulative wind hours and soil wind erosion mass. Cumulative wind hours were generated by computing the sum of all hours of critical wind velocity that lead to soil wind erosion over four years. In this paper, the critical wind velocity that leads to soil wind erosion is greater than 5 $m \cdot s^{-1}$. Therefore, the cumulative wind hour is the sum of all hours exhibiting a wind velocity greater than this value over four years. The spatial patterns of cumulative wind hour ($\geqslant 5$ $m \cdot s^{-1}$) and the mean of soil wind erosion moduli over four years are shown in Fig. 8. We can see that the spatial patterns of cumulative wind hour and the mean of soil wind erosion moduli match quite well. The cumulative wind hour was high in Wuzhai Country, Yanggao Country, Datong County, and the Nanjiao district, coinciding with peaks of the soil wind erosion in these areas. On the contrary, the intensity of soil

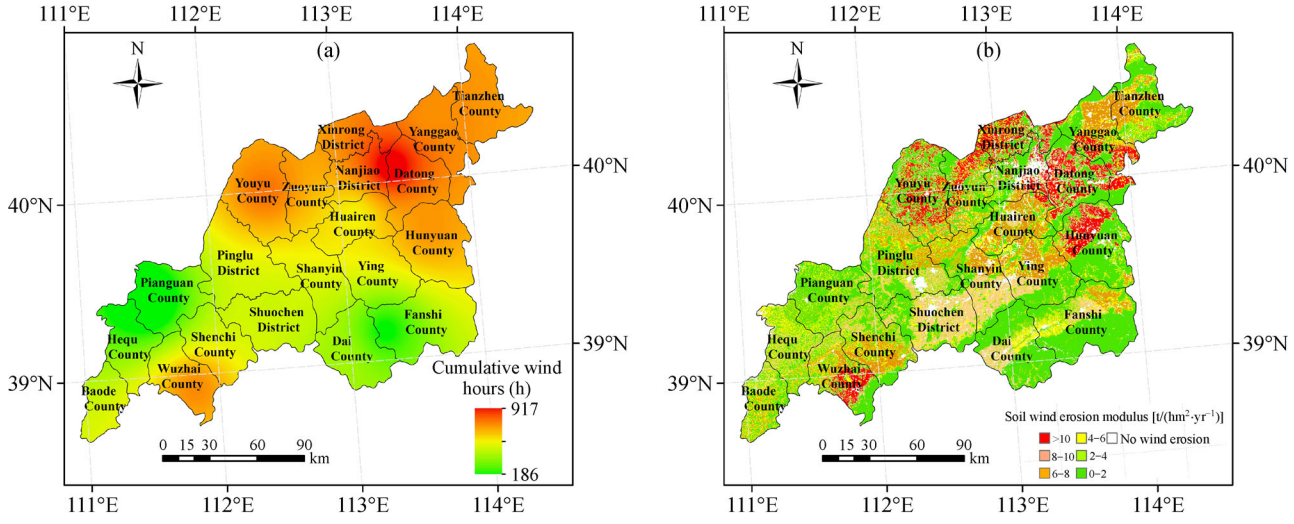

Fig. 8 (a) Spatial patterns of cumulative wind hour ($\geqslant 5$ m·s^{-1}) and (b) the mean of soil wind erosion modulus over 4 years.

erosion decreases in regions with less cumulative wind hours. We analyzed the interannual variations of soil wind erosion mass and cumulative wind hour (Fig. 9(a)). We also found that the cumulative wind hour fluctuations were well correlated with soil wind erosion mass. In 2001 and 2010, the soil wind erosion mass was relatively high, coinciding with the peak cumulative wind hours. Meanwhile, the soil wind erosion mass minima in 2005 and 2014 corresponded with cumulative wind hour minima for these years. Furthermore, the inter-annual variations of the different levels in wind cumulative hours were analyzed for northern Shanxi Province for the studied years (Fig. 9 (b)). Regionally, the decrease in soil wind erosion was a result of the decreased cumulative wind hours, especially for wind velocities of 5–8 m·s^{-1}. Therefore, wind was likely the main factor in regards to the decreased soil wind erosion mass across the northern Shanxi Province.

5 Conclusions

In this study, long-term remote sensing data and modeling data from 2000 to 2014 were used to illustrate vegetation and soil wind erosion dynamics of sandstorm control programs in the agro-pastoral transitional zone of northern China. Our results indicated that following the implementation of sandstorm control programs in 2000, the overall vegetation coverage increased and the soil wind erosion mass decreased. This means that the ecological effects of the sandstorm control programs were beneficial in northern Shanxi Province in the short term. The main conclusions are as follows:

1) Vegetation activity increased by 18.10% in northern Shanxi Province from 2000 to 2014 with a trend of 0.00346 yr^{-1}. 91.58% of the study area showed an increased NDVI, of which 63.59% had a significant

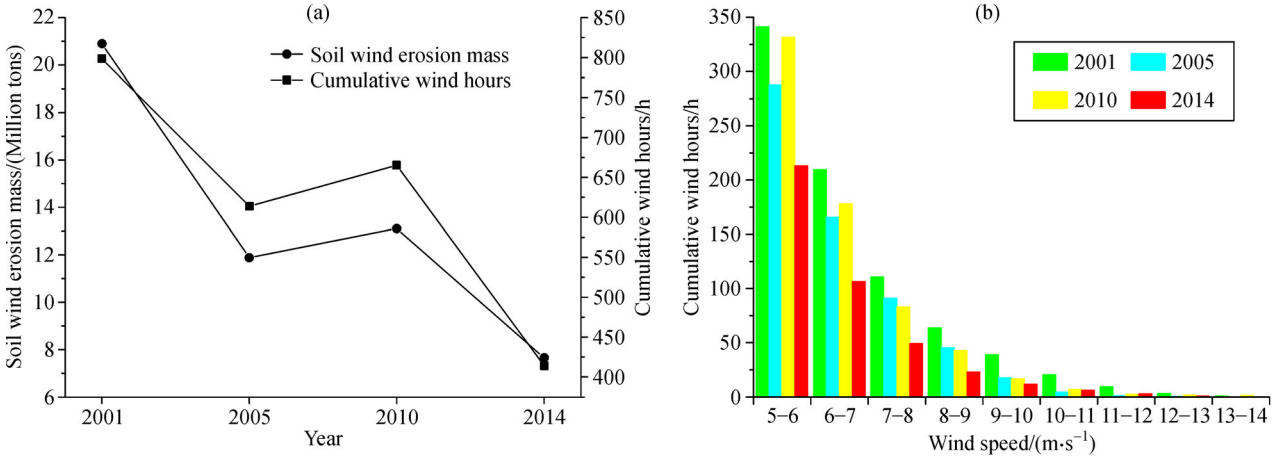

Fig. 9 (a) Interannual variations of soil wind erosion mass and cumulative wind hours and (b) the different levels of wind velocity cumulative hours in 4 years.

increase at the 0.95 confidence level. Spatially, the NDVI increased in the southwest, central, and northeast while it decreased sharply in the center of the Nanjiao district, southern Fanshi County, and northern Shuochen district. Seasonally, the greatest increase in NDVI occurred in the autumn.

2) Soil wind erosion mass has been reduced since the implementation of ecological restoration programs. Soil wind erosion mass decreased from 20.90 Mt in 2001 to 7.65 Mt in 2014. Compared with 2001, the soil wind erosion moduli decreased by 43.05%, 36.16%, and 62.66% in 2005, 2010, and 2014, respectively. Generally, the degree of soil wind erosion varied between regions. Soil wind erosion in most of study area has been reduced since 2001, in particular in Wuzhai and Youyu Counties.

3) The sandstorm control programs in northern Shanxi Province increased vegetation coverage and reduced dust by controlling soil wind erosion. Moreover, variations in ecological effects in the ecological restoration program region have also been linked with changes in wind.

Acknowledgements The authors are grateful to the Editor and anonymous reviewers of this paper. This research received financial supports from the Natural Science Foundation of Shanxi Province (No. 201701D221216) and National Natural Science Foundation of China (Grant Nos. 41401643 and 41475050).

References

Cao S (2008). Why large-scale afforestation efforts in China have failed to solve the desertification problem. Environ Sci Technol, 42(6): 1826–1831

Chen J, Chen Y, He C, Shi P (2001). Sub-pixel model for vegetation fraction estimation based on land cover classification. Journal of Remote Sensing, 5(6): 416–422

Deng L, Shangguan Z P, Rui L (2012). Effects of the Grain-for-Green Program on soil erosion in China. Int J Sediment Res, 27(1): 120–127

Donohue R J, Mcvicar T R, Roderick M (2009). Climate-related trends in Australian vegetation cover as inferred from satellite observations, 1981–2006. Glob Change Biol, 15(4): 1025–1039

Du Z Q, Xu X M, Zhang H, Wu Z T, Liu Y (2016). Geographical detector-based identification of the impact of major determinants on aeolian desertification risk. PLoS One, 11(3): e0151331

Fang J Y, Piao S L, He J, Ma W (2004). Increasing terrestrial vegetation activity in China, 1982–1999. Sci China Life Sci, 47(3): 229–240

Fensholt R, Proud S R (2012). Evaluation of earth observation based global long term vegetation trends–Comparing GIMMS and MODIS global NDVI time series. Remote Sens Environ, 119(3): 131–147

Fryrear D W, Saleh A, Bilbro J D (1998). A single event wind erosion model. Trans ASAE, 41(5): 1369–1374

Gao S Y, Zhang C L, Zhou X Y, Wu Y Q (2012). Benefits of Beijing-Tianjin Sand Source Control Engineering (2nd ed). Beijing: Science Press, 62–90

Gregory J M, Wilson G R, Singh U B, Darwish M M (2004). TEAM: integrated, process-based wind-erosion model. Environ Model Softw, 19(2): 205–215

Hagen L (1991). A wind erosion prediction system to meet the user needs. J Soil Water Conserv, 46(2): 107–111

He B, Chen A, Wang H, Wang Q F (2015). Dynamic response of satellite-derived vegetation growth to climate change in the Three North Shelter Forest Region in China. Remote Sens, 7(8): 9998–10016

Holben B N (1986). Characteristics of maximum value composite images from temporal AVHRR data. Int J Remote Sens, 7(11): 1417–1434

Lamchin M, Lee J, Lee W, Lee E J, Kim M, Lim C, Choi H, Kim S (2016). Assessment of land cover change and desertification using remote sensing technology in a local region of Mongolia. Adv Space Res, 57(1): 64–77

Liu D, Chen Y, Cai W, Dong W, Xiao J, Chen J, Zhang H, Xia J, Yuan W (2014). The contribution of China's Grain to Green Program to carbon sequestration. Landsc Ecol, 29(10): 1675–1688

Liu J, Li S, Ouyang Z, Tam C, Chen X (2008). Ecological and socioeconomic effects of China's policies for ecosystem services. Proc Natl Acad Sci USA, 105(28): 9477–9482

Liu L Y, Li X Y, Shi P J, Gao S Y, Wang J H, Ta W Q, Song Y, Liu M X, Wang Z, Xiao B L (2007). Wind erodibility of major soils in the farming-pastoral ecotone of China. J Arid Environ, 68(4): 611–623

Nan L, Du L T, Wang R (2013). Reviews on development of soil wind erosion models. World Science Technology Research & Development, 35(4): 505–509 (in Chinese)

Pi H, Sharratt B, Feng G, Lei J (2017). Evaluation of two empirical wind erosion models in arid and semi-arid regions of China and the USA. Environ Model Softw, 91: 28–46

Piao S L, Fang J Y, Zhou L M, Guo Q, Henderson M, Ji W, Li Y, Tao S (2003). Interannual variations of monthly and seasonal normalized difference vegetation index (NDVI) in China from 1982 to 1999. J Geophys Res, 108(D14): 4401–4413

Shao Y, Raupach M, Shortd D (1994). Preliminary assessment of wind erosion patterns in the Murray Darling Basin Australia. Recomb DNA Tech Bull, 47(3): 323–339

Shen X Y (2016). Temporal and Spatial Changes of Ecosystem Service and Tradeoff Analysis in Desertification Area of Northern Shanxi. Dissertation for Master Degree. Taiyuan: Shanxi University (in Chinese)

Slayback D A, Pinzon J E, Los S O, Tucker C J (2003). Northern hemisphere photosynthetic trends 1982–1999. Glob Change Biol, 9 (1): 1–15

Tian H, Cao C, Chen W, Bao S, Yang B, Myneni R B (2015). Response of vegetation activity dynamic to climatic change and ecological restoration programs in Inner Mongolia from 2000 to 2012. Ecol Eng, 82(4): 276–289

Tu Z, Li M, Sun T (2016). The status and trend analysis of desertification and sandification. Forest Resources Management, 2(1): 1–5 (in Chinese)

Wang J, Peng J, Zhao M, Liu Y, Chen Y (2017a). Significant trade-off for the impact of Grain-for-Green Programme on ecosystem services in North-western Yunnan, China. Sci Total Environ, 574: 57–64

Wang T (2014). Aeolian desertification and its control in Northern China. International Soil and Water Conservation Research, 2(4): 34–41

Wang X, Piao S, Ciais P, Li J, Friedlingstein P, Koven C, Chen A (2011). Spring temperature change and its implication in the change of

vegetation growth in North America from 1982 to 2006. Proc Natl Acad Sci USA, 108(4): 1240–1245

Wang X M, Zhang C X, Hasi E, Dong Z B (2010). Has the Three Norths Forest Shelterbelt Program solved the desertification and dust storm problems in arid and semiarid China? J Arid Environ, 74(1): 13–22

Wang Y, Liu L, Shangguan Z (2017b). Carbon storage and carbon sequestration potential under the Grain for Green Program in Henan Province, China. Ecol Eng, 100: 147–156

Webb N P, Herrick J E, Van Zee J W, Courtright E M, Hugenholtz C H, Zobeck T M, Okin G S, Barchyn T E, Billings B J, Boyd R, Clingan S D, Cooper B F, Duniway M C, Derner J D, Fox F A, Havstad K M, Heilman P, LaPlante V, Ludwig N A, Metz L J, Nearing M A, Norfleet M L, Pierson F B, Sanderson M A, Sharratt B S, Steiner J L, Tatarko J, Tedela N H, Toledo D, Unnasch R S, Van Pelt R S, Wagner L (2016). The national wind erosion research network: building a standardized long-term data resource for aeolian research, modeling and land management. Aeolian Res, 22: 23–36

Woodruff N, Siddoway F (1965). A wind erosion equation. Soil Sci Soc Am J, 29(5): 602–608

Wu J J, Zhao L, Zheng Y T, Lü A F (2012). Regional differences in the relationship between climatic factors, vegetation, land surface conditions, and dust weather in China's Beijing-Tianjin Sand Source Region. Nat Hazards, 62(1): 31–44

Wu Z T, Wu J J, He B, Liu J H, Wang Q F, Zhang H, Liu Y (2014). Drought offset ecological restoration program-induced increase in vegetation activity in the Beijing-Tianjin Sand Source Region, China. Environ Sci Technol, 48(20): 12108–12117

Wu Z T, Wu J J, Liu J H, He B, Lei T J, Wang Q F (2013). Increasing terrestrial vegetation activity of ecological restoration program in the Beijing-Tianjin Sand Source Region of China. Ecol Eng, 52(52): 37–50

Xu X M, Du Z Q, Zhang H (2016). Integrating the system dynamic and cellular automata models to predict land use and land cover change. Int J Appl Earth Obs Geoinf, 52: 568–579

Xue Z J, Qin Z D, Li H, Ding G, Meng X (2013). Evaluation of aeolian desertification from 1975 to 2010 and its causes in northwest Shanxi Province, China. Global Planet Change, 107(7094): 102–108

Yin R, Yin G (2010). China's primary programs of terrestrial ecosystem restoration: initiation, implementation, and challenges. Environ Manage, 45(3): 429–441

Zhang B, He C, Burnham M, Zhang L (2016). Evaluating the coupling effects of climate aridity and vegetation restoration on soil erosion over the Loess Plateau in China. Sci Total Environ, 539: 436–449

Zhang P, Shao G, Zhao G, Le Master D C, Parker G R, Dunning J B, Li Q (2000). China's forest policy for the 21st century. Science, 288 (5474): 2135–2136

Zhu S Z (2014). Vegetation dynamics in the desertification area of northern Shanxi Province based on the remote sensing data. Journal of Northeast Forestry University, 42(8): 69–74 (in Chinese)